Progress In Electromagnetics Research Letters, Vol. 98, 121–127, 2021

A Novel Planar Filtering Magic-T

Jun-Mei Yan*, Hai-Ying Zhou, and Liang-Zu Cao

Abstract—This paper presents a planar filtering magic-T with a simple structure. It consists of four half-wavelength microstrip resonators with one loaded with a shorted microstrip stub at its central location. The planar filtering magic-T has four ports, which all adopt a tapped line structure. Its novelty lies in the simple structure. Compared with previous works in the literature, its inter-resonator coupling zones are apart away and have no influence on each other, which means a simple design. Furthermore, a different-properties coupling is not needed, and its filtering response can be easily extended to the high-order case. The operational mechanism and design method are introduced in details. A planar filtering magic-T with center frequency of 920 MHz was designed and fabricated. The measured results show that, at the center frequency, the return loss (S_{11}/S_{44}) is less than 20/12 dB; an isolation degree of 25 dB (S_{41}) can be observed; the insertion losses of the difference port (S_{21}/S_{31}) and sum port (S_{24}/S_{34}) are 4.5/4.7 dB and 4.3/4.6 dB; the phase unbalance is $8^\circ/7^\circ(\Sigma/\Delta)$. Totally, these results can verify the effectiveness of the proposed novel planar filtering magic-T.

1. INTRODUCTION

The magic-T is an important microwave device, and it is applied in many aspects. In fact, magic-T can be seen as a device that integrates the functions of two power dividers. One has equal-magnitude and in-phase power division, and the other has equal-magnitude and out-of-phase power division. The two power dividers have common output ports. The input port of the power divider with equal-magnitude and in-phase power division is the so-called sum port or H port. The input port of the power divider with equal-magnitude and out-of-phase power division is the so-called difference port or E port. In the literature, many planar magic-T have been proposed [1–4]. These planar magic-T often involve multi-layer printed circuit board technology and need etch slot-line in the middle metal layer, which results in a complicated fabrication process.

Recently, the research for integrating filtering function into other microwave devices has received extensive interest. Also many new planar magic-T structures with filtering function have been proposed [5–12]. A typical planar filtering magic-T consists of four coupled resonators with loop-type coupling scheme. To realize the difference port, in some structures [5–10], a different-properties coupling is needed in the loop-type coupling structure (one electric coupling and three magnetic couplings or one magnetic coupling and three electric couplings). Another approach realizing the difference port is to utilize the odd-symmetry of the fundamental resonant mode in the half-wavelength microstrip resonator [11, 12]. Although the former has a compact size, its coupling zones are close and have an influence on each other. Furthermore, different-properties couplings must be introduced. These features increase the complexity of designing and implementing the planar filtering magic-T. The latter also has a deficiency, i.e., its filtering response is difficult to be extended to the high-order case.

This paper presents a novel planar filtering magic-T. The new structure can overcome the above shortages. Its filtering response can be easily extended to the high-order case, and its coupling zones

Received 11 April 2021, Accepted 3 June 2021, Scheduled 24 June 2021
* Corresponding author: Jun-Mei Yan (yjmzhy@163.com).
The authors are with School of Mechanical and Electronic Engineering, Jingdezhen Ceramic Institute, China.

are apart and have no influence on each other. Furthermore, a different-properties coupling is not needed. These features give much convenience to the design and implement of the proposed planar filtering magic-T. The remaining part of this paper will introduce the proposed novel planar filtering magic-T from several aspects including structure, operational mechanism, design method, simulation, and experimental verification.

2. STRUCTURE AND OPERATIONAL MECHANISM

Figure 1 gives the geometry configuration of the proposed planar filtering magic-T and its coupling scheme. The planar filtering magic-T is constructed by four half-wavelength microstrip-line resonators. Ports P_1 to P_4 are tapped with resonators R_1 to R_4, respectively. Port P_1 is the so-called difference port, and Port P_4 is the so-called sum port. The whole structure is symmetrical if port P_1 is not considered. For resonator R_1, the value of $2(L_1 + L_3 + L_4 + L_5 + L_6)$ should be equal to the half-wavelength at the center frequency. Similarly, for resonators R_2 and R_3 (both have the same physical dimensions), the value of $2L_6 + 2L_7 + 2L_8 + 4L_9 + L_{11}$ should also equal the half-wavelength at the center frequency. Resonator R_4 is loaded with a shorted stub (L_{15}) at its central location. The value of $L_6 + L_{12} + L_{13} + L_{16} + L_{14} + L_{15}$ should be equal to quarter-wavelength of the center frequency.

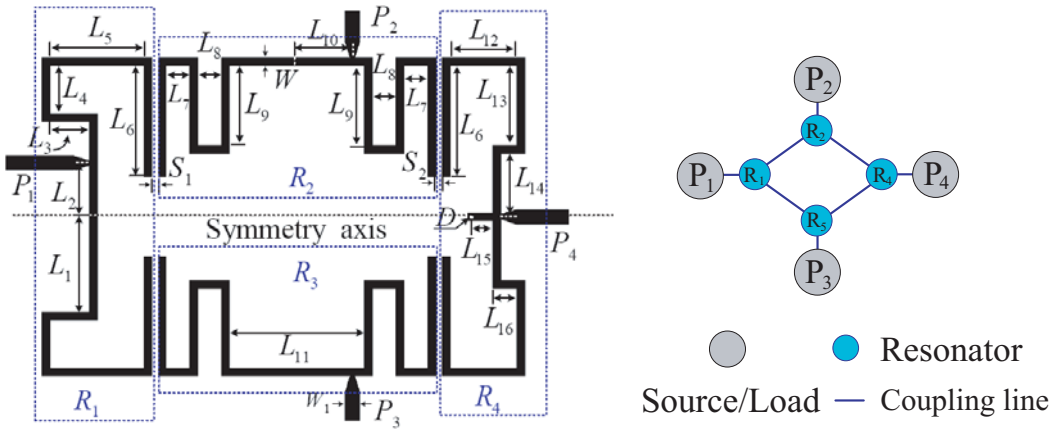

Figure 1. Layout of the proposed planar filtering magic-T and its coupling scheme.

Figure 2 shows the voltage distribution of the fundamental resonant mode of the resonators, and the external tapped line is included. Just as shown in Figure 2, resonators R_1, R_2, R_3 have odd-symmetry resonant mode. Both ends of the resonators have out-of-phase voltages, and the voltage at

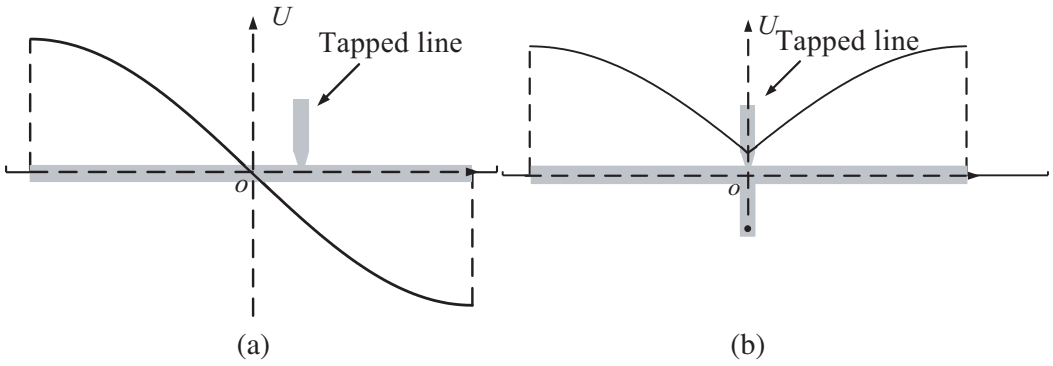

Figure 2. Voltage distribution of the fundamental resonant mode of the resonators. (a) For resonators R_1, R_2 and R_3. (b) For resonator R_4.

its central location is zero. The tapped point of the external port is deviated from the central location. The resonator R_4 has even-symmetry resonant mode, and its both ends have in-phase voltages. The voltage of its central location is non-zero. The tapped point of the external port is located at the central location.

Resonator R_1 has out-of-phase voltage distribution at its both ends when signal is input from port P_1 (difference port), which results in that resonators R_2 and R_3 have opposite voltage distributions. Thus ports P_2 and P_3 output equal-magnitude and out-of-phase signals, i.e., the differential-mode signals. Their signal polarity is shown in Figure 3(a). Although resonator R_4 is excited by resonators R_2 and R_3, it will not resonate because its resonant mode is even-symmetry. The excitations from resonators R_2 and R_3 are the differential-mode signals. Thus, port P_4 has no output signal, i.e., there is an isolation feature between ports P_1 and P_4.

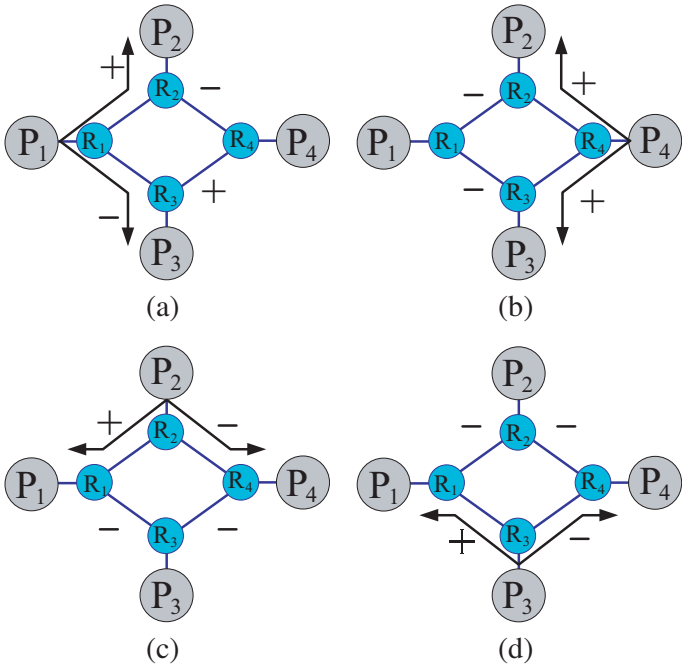

Figure 3. Various signal polarity when signal is inputted from (a) port P_1, (b) port P_4, (c) port P_2 and (d) port P_3.

However when signal is input from port P_4 (sum port), resonator R_4 has in-phase voltage at its both ends, which results in that resonators R_2 and R_3 have in-phase voltage distributions. Thus, ports P_2 and P_3 output equal-magnitude and in-phase signals, i.e., the common-mode signals. Their signal polarity is shown in Figure 3(b). Although resonator R_1 is excited by resonators R_2 and R_3, it will not resonate because its resonant mode is odd-symmetry. The excitations from resonators R_2 and R_3 are the common-mode signals. Thus, port P_4 has no output signal, i.e., there is an isolation feature between ports P_1 and P_4.

Figures 4(a) and 4(d) show the simulated surface current distributions (vector plots) when signal is input from ports P_1 and P_4, respectively. When port P_1 is excited, the current is dominant on resonators R_1, R_2, and R_3, and currents on resonators R_2 and R_3 are odd-symmetry. The blue arrows indicate the current directions at ports P_2 and P_3, which are out-of-phase. When port P_4 is excited, the current is dominant on resonators R_4, R_2, and R_3, and currents on resonators R_2 and R_3 are even-symmetry. The blue arrows indicate the current directions at ports P_2 and P_3, which are in-phase. The simulated results show that there is an isolation feature between ports P_1 and P_4.

In fact, port P_2/P_3 can also be seen as the difference/sum port. When signal is input from port P_2, resonator R_2 has out-of-phase voltage at its both ends, which results in that ports P_1 and P_4 output equal-magnitude and out-of-phase signals, i.e., the difference-mode signals. Their signal polarity is

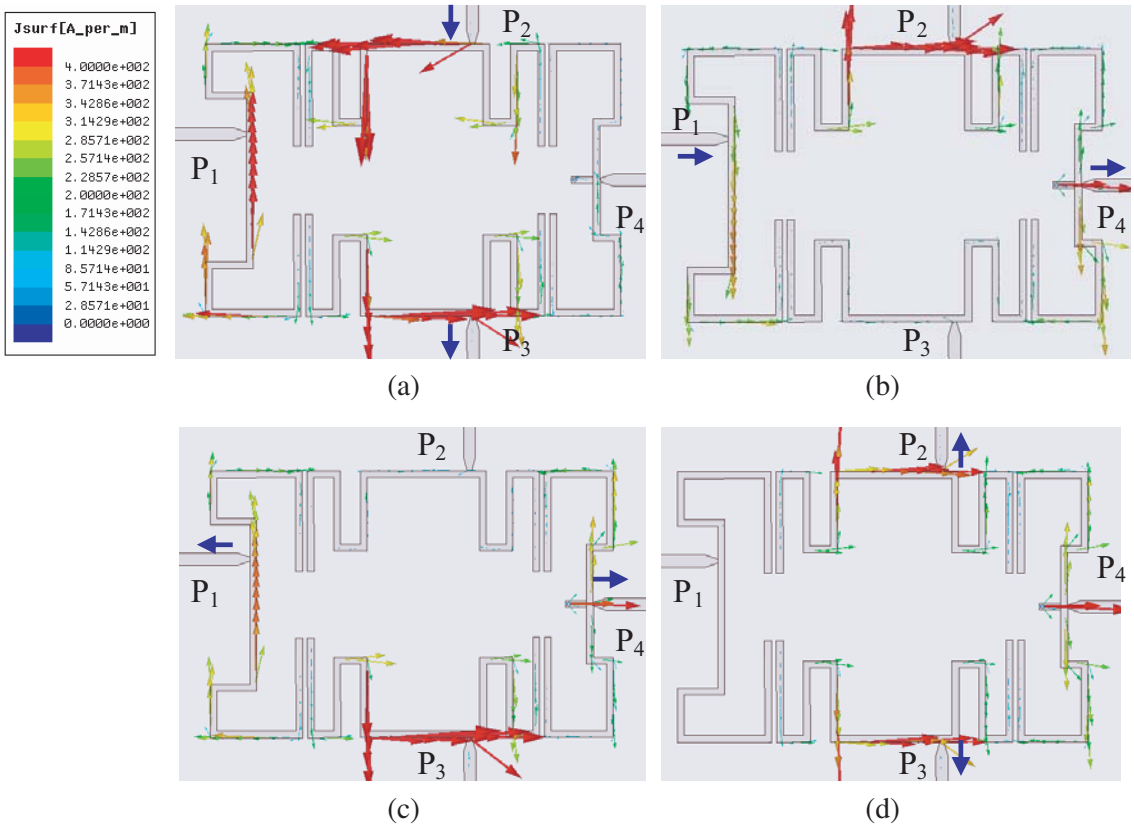

Figure 4. The simulated surface current distribution (vector plots) when various ports are excited (The blue arrows indicate the current direction at the respective port). (a) P_1 is excited. (b) P_2 is excited. (c) P_3 is excited. (d) P_4 is excited.

shown in Figure 3(c). Although resonator R_3 is excited by resonators R_1 and R_4, it will not resonate because its resonant mode is odd-symmetry. While the excitations from resonators R_1 and R_4 are the common-mode signals. Thus port P_3 has no output signal, i.e., there is an isolation feature between ports P_2 and P_3. However when signal is input from port P_3, resonator R_3 has out-of-phase voltage at its both ends, which results in that ports P_1 and P_4 output equal-magnitude and in-phase signals, i.e., the common-mode signals. Their signal polarity is shown in Figure 3(d). Although resonator R_2 is excited by resonators R_1 and R_4, it will not resonate because its resonant mode is odd-symmetry, while the excitations from resonators R_1 and R_4 are the common-mode signals. Thus port P_3 has no output signal, i.e., there is an isolation feature between ports P_2 and P_3.

Figures 4(b) and 4(c) show the simulated surface current distribution (vector plots) when signal is input from ports P_2 and P_3, respectively. When port P_2 is excited, the current is dominant on resonators R_2, R_1, and R_4. The blue arrows indicate the current direction at ports P_1 and P_4, which are out-of-phase. When port P_3 is excited, the current is dominant on resonators R_3, R_1, and R_4. The blue arrows indicate the current directions at ports P_1 and P_4, which are in-phase. The simulated results show that there is an isolation feature between ports P_2 and P_3. Totally, the simulated results of the surface current distribution verify the operational mechanism of the planar filtering magic-T.

Compared with some previous structures [5–10] in the literature, the couplings between resonators in the proposed structure are all electric coupling, and no coupling with different properties is needed. Furthermore, all the electric couplings occur at the zones between the ends of the resonators, which results in a sufficient distance between the coupling zones. Thus influence between coupling zones does not exist. These features give much convenience to designing and implementing the proposed planar filtering magic-T. Additionally, if a high-order filtering response is needed, what is only needed to do is to insert resonators in the loop-type coupling scheme.

3. DESIGN

This proposed planar filtering magic-T can be designed by utilizing the conventional bandpass-filter design method with a simple modification. The design steps are as follows. Firstly, lengths of the microstrip resonators are determined based on the central frequency. Secondly, element values g_0, g_1, g_2, g_3 of the prototype low-pass filter are obtained based on the filtering specifications (Return loss and Fractional bandwidth) [13], then, the external quality factors and internal coupling coefficients can be calculated according to the following formulas,

$$Q_{e1} = \frac{g_0 g_1}{FBW}, \qquad Q_{e2} = \frac{g_2 g_3}{FBW} \tag{1}$$

$$M_{12} = \frac{FBW}{\sqrt{g_1 g_2}} \tag{2}$$

where FBW is the fractional bandwidth. Thirdly, the coupling coefficient should be modified as $M_{12}/\sqrt{2}$ [8]. Fourthly, the port quality factors and inter-resonator coupling coefficients can be extracted based on the extraction approaches proposed in [14]. Thus, the initial physical dimensions of the resonators and coupling structure can be determined. Lastly, the field simulation of the whole structure is conducted. Generally speaking, the performance does not satisfy the required specifications. Now a few tuning works are needed. According to above steps, a planar magic-T with second-order bandpass filtering response with center frequency of 920 MHz, insertion loss of 0.01 dB, and FBW of 2.0% is designed. Its low-pass element values is $g_0 = 1.0$, $g_1 = 0.4489$, $g_2 = 0.4078$, $g_3 = 1.1008$. The port quality factors and inter-resonators coupling coefficient are $Q_{e1} = Q_{e2} = 22.4$ and $M_{12} = 0.04674$. The modified coupling coefficient is $M_{12}/\sqrt{2} = 0.03305$.

4. IMPLEMENTATION AND DISCUSS

To demonstrate the novel planar filtering magic-T and its design method, a second-order filtering planar magic-T with center frequency of 920 MHz and fractal bandwidth of 2.0% has been designed, fabricated, and measured. The used Rogers4003C substrate has thickness of 0.81 mm, relative dielectric constant of 3.55, and loss tangent of 0.002. The vector network analyzer (Agilent E5071B) is used for measurement, and HFSS 15.0 is used as the field simulation tool. The layout is shown in Figure 1, and its physical

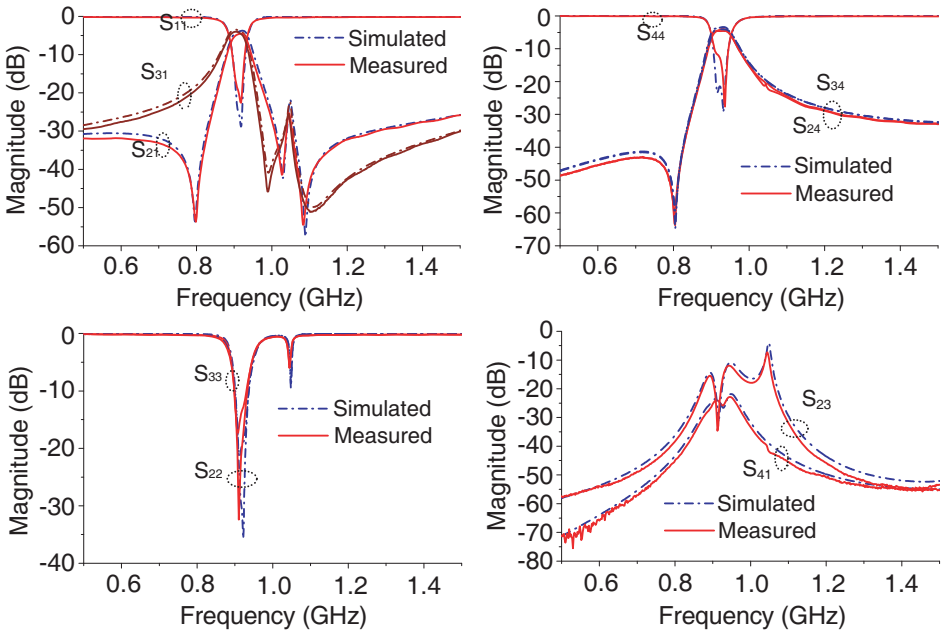

Figure 5. Simulated and measured magnitude results of the fabricated filtering planar magic-T.

dimensions are as follows (units mm): $W_1 = 1.8$, $W = 1.0$, $L_1 = 12.0$, $L_2 = 6.8$, $L_3 = 5.0$, $L_4 = 6.0$, $L_5 = 11.9$, $L_6 = 14.0$, $L_7 = 3.0$, $L_8 = 3.0$, $L_9 = 11.0$, $L_{10} = 7.0$, $L_{11} = 17.0$, $L_{12} = 8.4$, $L_{13} = 10.0$, $L_{14} = 8.0$, $L_{15} = 2.0$, $L_{16} = 3.0$, $D = 0.5$, $S_1 = 0.74$, $S_2 = 0.72$. Diameter of the via hole is 0.5. The total size is $40.0 \times 60.0\,\text{mm}^2$, about $0.2 \times 0.3\lambda_g^2$, where λ_g is the guided wavelength of a 50-Ohm microstrip line at the center frequency. Figure 4 shows the simulated surface current distributions (vector plots) at the center frequency, and they have been discussed in the above section. Figure 5 and Figure 6 give the simulated and measured results. A photograph of the fabricated planar filtering magic-T is also shown as inset in Figure 6. At the center frequency, the measured return loss (S_{11}/S_{44}) is less than 20/12 dB. An isolation degree of 25 dB (S_{41}) can be observed. The insertion losses of the difference port (S_{21}/S_{31}) and sum port (S_{24}/S_{34}) are 4.5/4.7 dB and 4.3/4.6 dB. Apart from the inherent 3 dB due to the power division, the insertion loss is mainly from the dielectric loss and radiation loss. The phase unbalance is $8°/7°(\Sigma/\Delta)$. The simulated and measured results have a good agreement, which verifies the effectiveness of the proposed filtering planar magic-T and its design method.

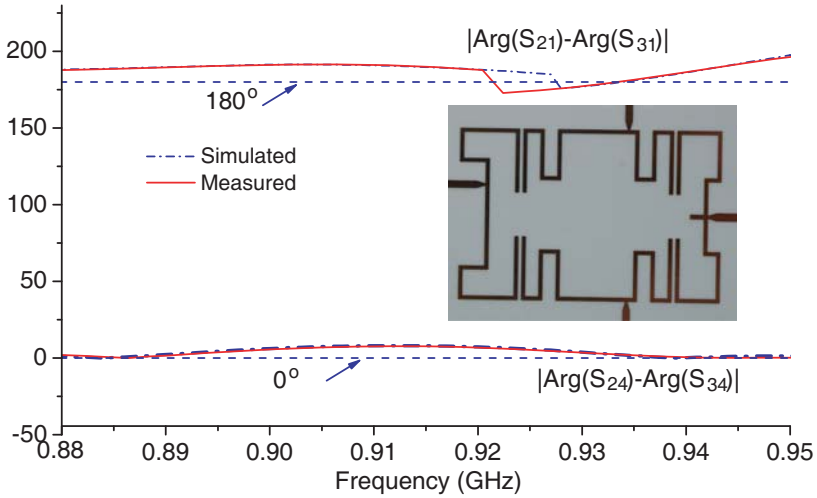

Figure 6. Simulated and measured phase results and photograph of the fabricated planar filtering magic-T.

5. CONCLUSION

A novel planar filtering magic-T and its design method are presented in this letter. Its novelty lies in a simple structure. Its coupling zones are apart and have no influence on each other. A different-properties coupling is not needed in the loop-type coupling scheme. These features give much convenience to designing and implementing the proposed planar filtering magic-T. Furthermore, its filtering response can be easily extended to the high-order case. Its geometry configuration and operation mechanism have been described in details. The conventional bandpass filter design method based on the coupling matrix can be applied here with only a simple modification. The detailed design steps have been given. A prototype filtering planar magic-T has be designed, fabricated, and measured. The simulated and measured results have a good agreement, which verifies the effectiveness of the filtering planar magic-T and its design method.

ACKNOWLEDGMENT

This work is supported by the National Natural Science Foundation of China (grant No. 61741110, 61661023).

REFERENCES

1. Katsube, M. W., Y. M. M. Antar, A. Ittipiboon, and M. Cuhaci, "A novel aperture coupled microstrip 'magic-T'," *IEEE Microw. Wireless Compon. Lett.*, Vol. 2, No. 6, 245–246, 1992.
2. Kim, J. P. and W. S. Park, "Novel configurations of planar multilayer magic-T using microstrip-slotline transitions," *IEEE Trans. Microw. Theory Techn.*, Vol. 50, No. 7, 1683–1688, 2002.
3. He, F. F., K. Wu, W. Hong, H. J. Tang, H. B. Zhu, and J. X. Chen, "A planar magic-T using substrate integrated circuits concept," *IEEE Microw. Wireless Compon. Lett.*, Vol. 18, No. 6, 386–388, 2008.
4. Yen, K. U., E. J. Wollack, J. Papapolymerou, and J. Laskar, "A broadband planar magic-T using microstrip-slotline transitions," *IEEE Trans. Microw. Theory Techn.*, Vol. 56, No. 1, 172–177, 2008.
5. Wang, W., T. Shen, T. Huang, and R. Wu, "Miniaturized rat-race coupler with bandpass response and good stopband rejection," *2009 IEEE MTT-S International Microwave Symposium Digest*, 709–712, 2009.
6. Chen, C., J. Li, G. Wang, K. Zhou, and R. Chen, "Design of compact filtering 180-degree hybrids with arbitrary power division and filtering response," *IEEE Access*, Vol. 7, 18521–18530, 2019.
7. Chen, C., T. Huang, C. Chen, W. Liu, T. Shen, and R. Wu, "A compact filtering rat-race coupler using dual-mode stub-loaded resonators," *2012 IEEE MTT-S International Microwave Symposium Digest (MTT)*, 1–3, 2012.
8. Liu, W., T. Huang, C. Chen, T. Shen, and R. Wu, "Design of a 180-degree hybrid with Chebyshev filtering response using coupled resonators," *2013 IEEE MTT-S International Microwave Symposium Digest (MTT)*, 1–3, 2013.
9. Lin, T.-W., J.-Y. Wu, and J.-T. Kuo, "Filtering rat-race coupler with transmission zeros using compact miniaturized hairpin resonators," *2015 IEEE International Wireless Symposium (IWS 2015)*, 1–4, 2015.
10. Lin, C. and J. Kuo, "Compact eighth-order microstrip filtering coupler," *2017 IEEE Asia Pacific Microwave Conference (APMC)*, 806–808, 2017.
11. Lin, C. and S. Chung, "A compact filtering 180° hybrid," *IEEE Trans. Microw. Theory Techn.*, Vol. 59, No. 12, 3030–3036, 2011.
12. Wang, K., X. Y. Zhang, S. Y. Zheng, and Q. Xue, "Compact filtering rat-race hybrid with wide stopband," *IEEE Trans. Microw. Theory Techn.*, Vol. 63, No. 8, 2550–2560, 2015.
13. Matthaei, G. L., L. Young, and E. M. T. Jones, *Microstrip Filter, Impedance-matching Networks and Coupling Structures*, Artech House, Norwood, MA, 1980.
14. Hong, J. S. and M. J. Lancaster, *Microstrip Filter for RF/Microwave Applications*, John Wiley & Sons, 2001.